Short Communication

Synthesis and Characterisation of slow pyrolysis Pine Cone bio-char in the removal of organic and inorganic pollutants from aqueous solution by adsorption: Kinetic, equilibrium, mechanism and thermodynamic

Sara. Dawood, Tushar Kanti Sen, Chi Phan

PII: S0960-8524(17)31105-7
DOI: http://dx.doi.org/10.1016/j.biortech.2017.07.019
Reference: BITE 18438

To appear in: *Bioresource Technology*

Received Date: 28 May 2017
Revised Date: 30 June 2017
Accepted Date: 4 July 2017

Please cite this article as: Dawood, Sara., Sen, T.K., Phan, C., Synthesis and Characterisation of slow pyrolysis Pine Cone bio-char in the removal of organic and inorganic pollutants from aqueous solution by adsorption: Kinetic, equilibrium, mechanism and thermodynamic, *Bioresource Technology* (2017), doi: http://dx.doi.org/10.1016/j.biortech.2017.07.019

Synthesis and Characterisation of slow pyrolysis Pine Cone bio-char in the removal of organic and inorganic pollutants from aqueous solution by adsorption: Kinetic, equilibrium, mechanism and thermodynamic

Sara. Dawood [a], Tushar Kanti Sen [b*], Chi Phan [c]

Department of Chemical Engineering, Curtin University, GPO Box U1987, 6845 WA, Australia.

Email address: sara.dawood@postgrad.curtin.edu.au [a]

Email address: t.sen@curtin.edu.au [b]

Email address: c.phan@curtin.edu.au [c]

[*]Corresponding author's email: t.sen@curtin.edu.au

Abstract

Pine cone bio-char was synthesised through slow pyrolysis at 500˚C, characterized and used as an effective adsorbent in the removal of organic Methylene Blue (MB) dye and inorganic nickel metal (Ni(II) ions from aqueous phase. Batch adsorption kinetic study was carried out by varying solution pH, dye concentration, temperature, adsorbent dose and contact time. Kinetic and isotherm models indicates that the adsorption of both adsorbates onto pine cone bio-char were mainly by chemisorption. Langmuir maximum adsorption capability was found to be 106.4 and 117.7 mg/g for methylene blue (MB) and nickel ions (NI(II) respectively. Thermodynamic parameters suggested that the adsorption was an endothermic and spontaneous. These results indicate the applicability of pine cone as a cheap precursor for the sustainable production of cost-effective and environmental friendly bio-char adsorbent.

Keywords: Bio-char, pine cone, Methylene Blue, nickel, adsorption.

1 Introduction

Bio-char is a pyrogenic carbonaceous material produced from various biomass residue and woody materials in an oxygen-limited atmosphere while charcoal can be produced from animal or biomass in absence of oxygen (Hardy et al., 2017). Bio-char is used in various applications such as in soil treatment, building materials, medical uses, pollution control, waste management and wastewater treatments due to its large surface area, porous structure and cost-effective synthesis process (Zhang et al., 2017). Organic compounds such as dyes are widely used in textile, printing, leather, cosmetic and paper industries (Dawood & Sen, 2012). Inorganic contaminations such as heavy metal are produced from refining, battery, electroplating and welding industries (Kara et al., 2017). The presence of these potential pollutants in water streams can cause serious environmental and health issues and therefore must be treated to permissible concentration limits before discharging into the water bodies. Commercial activated carbon (CAC) is proven to be an effective adsorbent in the removal of organic and inorganic pollutants dissolved in aqueous media or from gaseous environment (Dawood et al., 2014; Ribas et al., 2014). However, its high cost, non-renewable production source and difficulties with its regeneration have encouraged researchers to find alternative cost-effective adsorbents. Therefore, researchers are focusing upon the production of cost-effective charcoal and bio-char derived from agriculture solid wastes that can be used for removal of dyes and heavy metals form wastewater. There are many reported agriculture solid waste based char, charcoal , activated carbon and magnetic composite charcoal used in the removal of dyes and heavy metals such as bamboo bio-char (Liao et al., 2012), cocoa shell activated carbon (Ribas et al., 2014), pine cone

based activated carbon (Dawood et al., 2014), coconut pith char (Johari et al., 2016) , almond shell bio-char (Kılıç et al., 2013), Eucalyptus bark bio-char (Dawood et al., 2016), banana peel bio-char (Zhou et al., 2017), celery bio-char (Zhang et al., 2017), magnetic bamboo charcoal (Nomura et al., 2017) and Korean cabbage bio-char (Sewu et al., 2017). In this research study, pine cone (*Pinus radiata*) has been selected as a precursor material for the production of cost effective pine cone based bio-char. Therefore, the main objectives of this work are to synthesize bio-char from pine cone biomass and investigate its effectiveness in the removal of organic methylene blue (MB) dye and inorganic Ni (II) ions from aqueous solutions. The adsorption kinetics and mechanism of adsorption have also been identified here by batch kinetic and equilibrium adsorption study under various physico-chemical process parameters.

2 Materials and Methods

2.1 Adsorbate chemicals and measurement

All chemicals used were of analytical grade and obtained from Sigma Chemical Co. Stock solutions of 1000 mg/L MB dye and nickel metal ions ($Ni(NO_3)_2 \cdot 6H_2O$ salt) were prepared and stored respectively. The solution pH was adjusted by either 0.1M hydrochloric acid, 0.1M sodium hydroxide or 0.1M ammonium hydroxide solutions using a digital pH meter (PHTESTR30). The UV/VIS (V-670) spectrophotometer and AA-7000 Atomic Absorption Spectrophotometer (AAS) were used to measure the concentration of MB dye and Ni (II) metal ions respectively.

2.2. Synthesis of pine cone bio-char through slow pyrolysis and its characterization

Pine cones were collected from the Curtin University Bentley campus, Western Australia, Australia. The collected pine cones were washed several times with ultra-pure

water to remove impurities, dried at 75˚C overnight. Biochar was synthesized from dried pine cone biomass through slow pyrolysis in a muffle furnace under limited oxygen content and atmospheric pressure. The temperature profile was increased at the rate of 10˚C/min until it reached the set point of 500˚C and kept at the set point temperature for a period of 2.5 hrs. It was also reported that biomass based biochars produced at higher temperature exhibits high surface area, porosity and bulk density which may give higher adsorption capacity compared to low temperature biochars production (Dawood and Sen 2012, Dawood et al, 2014). The formed bio-char was cooled down gradually inside the furnace for a period of 5 hrs. The obtained bio-char was ground using a mechanical grinder (GmbH & Co. KG, West Germany) and used for experiments. The synthesized biochar was characterized by FTIR and BET analyser. C-H-N analysis was also conducted. Bulk density and bio-char yield were measured as per equation (1) and (2) respectively.

$$\text{Bulk Density} = \frac{\text{mass of dry sample(g)}}{\text{total volume used (ml)}} \quad (1)$$

$$\text{Yield (\%)} = \frac{w_c}{w_o} \text{ x } 100 \quad (2)$$

Where w_c is the dry weight (g) of the final bio-char and w_o is the dry weight (g) of pine cone biomass.

2.3. Batch adsorption experiments

Batch adsorption experiments were performed by shaking a mixture of a fixed amount of pine bio-char with 50 ml of adsorbate of a known concentration in a series of 125 ml plastic bottles as per our old method (Dawood & Sen, 2012b) in a constant temperature

shaker for a known period of time. The suspensions were taken out at predetermined time intervals and then filtered using micro filter of pore size 0.47 µm for Ni (II) and the filtrates were analysed using atomic absorption spectrophotometer. But for MB, the mixture were centrifuged and the residual MB concentration was measured by UV spectrophotometer. Several experiments were carried out by varying initial solution pH, contact time, adsorbent dose, initial dye concentration and temperature respectively. The amount of adsorbate adsorbed onto pine cone bio-char at time t, q_t (mg/g) and % adsorptive removal are calculated from equations (3) and (4) respectively. Also, equilibrium adsorption experiment was conducted with a wide range of MB dye and Ni (II) concentrations (10– 70 mg/L) contacted with 20 mg bio-char for an equilibrium time of 3.5 hrs at 35 ºC and at optimum solution pH

$$q_t = \frac{(C_o - C_t)V}{m} \quad (3)$$

$$\% \text{ Removal} = \frac{(C_o - C_t)}{C_o} \times 100 \quad (4)$$

Where C_o is the initial adsorbate concentration (mg/L), C_t is the concentration of adsorbate at any time t, V is the volume of adsorbate solution (0.05 L) and m is the mass of adsorbent in (g). All experimental measurements were within $\pm$10 % accuracy.

2. Results and discussion

2.2 Surface, elemental and morphological characterization of pine cone bio-char

Brunaer-Emmett-Teller (BET) surface area and the pore size diameter of synthesized biochar were found to be 335 m^2/g and 3.1 nm respectively. The bulk density was calculated as 0.54 g/cm^3 using equation (1). The American Water Work Association has set a lower limit on bulk density of 0.25 g/cm^3 for practical use thus indicates the

applicability of pine cone bio-char (Dawood and Sen 2014). Synthesis bio-char yield was calculated as 33.5%. Also, the point of zero charge (pH_{zpc}) was determined as per solid addition method (Nawaz et al., 2014) which was found as 8.5 from the plot pH $_{(initial)}$ vs. Δ pH $_{(initial-final)}$ which is not presented here. This indicates that pH < $pH_{pzc,}$ the surface of bio-char is predominantly positive in charge, where pH > pH_{pzc} the surface charge becomes negative in nature. Elemental analysis was performed by C-H-N analyser and the carbon content of pine bio-char was determined as 71.5%. The FTIR spectrum of the pine bio-char for which plot is not presented here indicates the presence of a peak band at 3416 cm^{-1} and this is due to O-H vibrations of alcohols, phenols and carboxylic acids presented in cellulose and lignin. Peaks also observed at 1710 cm^{-1} and 1581 cm^{-1} presented (C═O) stretching of carboxyl groups (COOH) thus indicate the existence of acidic oxygen containing functional groups that increase the adsorption capacity of heavy metals. Also presence of small peak shown at 700 cm^{-1} indicate the presence of phenyl group.

2.3 Effect of various physiochemical process parameters (solution pH, dose, initial adsorbate concentration and temperature) on MB dye and Ni (II) adsorption by synthesized biochar

Pine cone bio-char was used in the removal of MB dye and Ni (II) from aqueous solution under different initial solution pH (5.1-11.3) where the other parameters were kept constant as shown in Fig.1 (a). It was found that the amount of MB dye adsorbed, q_t (mg/g) and percentage dye removal were increased significantly with the increase in solution pH. Furthermore, the amount of Ni (II) adsorbed, q_t (mg/g) and metal ions removal efficiency was increased with the increase of solution pH from 5.1 to 9.4 then

decreased significantly at a solution pH of 11.3 as shown in Fig.1 (a). Initial solution pH higher than pH_{zpc} of 8.5, the stretching hydroxyl (–OH) and carboxyl (–COOH) groups presented on the surface of pine cone bio-char were deprotonated and became more negatively charged (Maneerung et al., 2016) .Therefore, the adsorption of both MB dye and Ni (II) on bio-char tends to increase rapidly due to the increase of electrostatic interaction of cationic dye and Ni (II) metal ions with the negatively charged pine cone bio-char surface to form a solid surface complex. However, as seen in Fig.1 (a), Ni (II) solution with pH higher than 9.4 decreases the amount of nickel ions adsorption and removal efficiency respectively. This may be due to the formation of soluble hydroxylated complexes of the nickel ions and their competition with the active sites of the bio-char surface. Acidic solution pH tends to decrease the adsorption capacity of both MB dye and Ni (II) onto bio-char due to presences of hydronium (H_3O^+) ions competing with the cationic dye and metal ions for the adsorption sites respectively.

Adsorbent dose is an important parameter for adsorber design. Therefore effect of various bio-char doses (10-50 mg /50 ml) in the removal of both MB dye and Ni (II) from aqueous solution keeping other parameters constant were studied and presented in Fig.1(b). It was observed from Fig.1 (b) that the increase in adsorbent dose resulted in decrease of amount of both adsorbed MB dye and Ni (II), q_t (mg/g), whereas the percentage removal of both the adsorbate was increased with the increase of adsorbent mass. The decrease in amount of adsorption, q_t (mg/g) with increasing adsorbent mass is due to the split in the flux or the concentration gradient between solute concentration in the solution and the solute concentration on the surface of the adsorbent (Dawood et al.,

2014). Low adsorbent dose, the adsorbate molecules are more easily accessible and hence the adsorbate removal per unit mass of adsorbent was high.

The effect of initial MB dye and Ni (II) concentrations and contact time were investigated and results are presented in Fig.1 (c) and (d) respectively. From Fig.1 (c), it was observed that the amount of MB dye adsorbed q_t (mg/g) increased rapidly from 21.9 mg/g to 82.2 mg/g with the increases of initial dye concentration (10-50 mg/L). Concurrently, percentage dye removal decreased from 87.5 % to 65.8% for the same initial concentration. Furthermore, the amount of Ni (II) ions adsorbed q_t (mg/g) increased from 20.1 mg/g to 77.1 mg/g with the increases of initial nickel ions concentration (10-50 mg/L) while the percentage removal efficiency decreased from 80.4 % to 61.7 % for the same initial concentration as shown in Fig.1 (c). The initial adsorbate concentration provides a high driving force to overcome the resistance to the mass transfer of adsorbate between the aqueous solution and the solid pine cone bio-char (Maneerung et al., 2016). Also, it was observed that the amount of adsorption q_t (mg/g) increases rapidly with contact time at all adsorbate initial concentrations and equilibrium is attained within 120 min as shown in Fig.1 (d). Fig. 1(d) also indicates that overall adsorption process is more or less two steps process where a very rapid adsorption of MB dye and Ni (II) occurred on the bio-char external surface followed by slow and intra-particle diffusion in the interior of the adsorbent surface (Afroze et al., 2016).

To investigate the effect of solution temperature, MB dye and Ni(II) batch adsorption studies on biochar were extended at three different temperatures of 25 to 45 ^{0}C. That amount of MB dye removal observed to increase from 57.5 % to 83.6 % and

the amount of Ni (II) removal increased from 61.2% to 78.2 % with the increases of temperature profiles (25-45°C) respectively and indicates the process becomes endothermic in nature. This may be due to increase of active sites and also due to increase the mobility of the adsorbate's molecules with increasing temperature. This was further supported by various thermodynamic parameters calculations. Change of Gibb's free energy (ΔG^0), entropy (ΔS^0) and enthalpy changes (ΔH^0) were calculated from well-known Van't Hoff equation and thermodynamic relationship between $\Delta G^{0,}$ ΔH^0 and ΔS^0 (Dawood and Sen, 2012). The obtained range of values of ΔG^0 lies between -20.7 KJ/mole to – 24.3 KJ/mole for Ni-char system at three different temperatures, whereas -3.4 KJ/mole to -7.4 KJ/mole were obtained for MB-char system. Similarly ΔH^0 of 32.68 KJ/mole and 56.3 KJ/mole were found at three different teperatures for Ni-Char and MB-Char system respectively. The positive values of ΔH^0 and negative values of ΔG^0 indicates the process becomes spontaneous and endothermic in nature.

2.4 Adsorption kinetics and mechanism of adsorption

The experimental data were applied to pseudo-first-order, pseudo-second-order and intra-particle diffusion models to determine the adsorption mechanism, and predicting the rate-controlling step in the adsorption of MB dye and Ni (II) on pine bio-char. The pseudo-first-order and pseudo-second-order rate equations are presented by following linear equations (5) and (6) respectively (Dawood and Sen, 2014).

$$\text{Log}\,(q_e - q_t) = \log q_e - \frac{k_f}{2.303}\,t \qquad (5)$$

$$\frac{t}{q_t} = \frac{1}{q_e}\,t + \frac{1}{k_s\,q_e^2} \qquad (6)$$

Where q_t (mg/ g) is the amount of adsorbate adsorbed at time t, q_e (mg/g) is the adsorption capacity at equilibrium. k_f (min^{-1}) and ks (g/mg.min) are the pseudo-first-order and pseudo-second-order rate constants. Intra-particle diffusion model was also used for identifying the adsorption mechanism, reaction and predicting the rate-controlling step (Weber & Morriss, 1963) and it is described as shown in equation (7)

$$q_t = k_{id}\, t^{0.5} + C \quad (7)$$

Where k_{id} (mg/g $min^{0.5}$) is the intra-particle diffusion rate constant and C (mg/g) is a constant associated with the thickness of the boundary layer. Higher value of constant C (mg/g) indicates a greater effect on the limiting boundary layer.

Further, Chi-square (χ^2) error test was performed to evaluate the accuracy of these kinetic models and determine the error between experimental ($q_{e)}$ and calculated (q_e) as shown in equation (8).

$$\chi^2 = \frac{(q_e \text{exp} - q_e \text{ calc})^2}{q_e \text{ calc}} \quad (8)$$

Pseudo-first-order, pseudo-second-order and intraparticle diffusion kinetic model parameters along with values of linear regression coefficients under various physicochemical process parameters are obtained from the respective fitted plots (plots are not presented here) which are tabulated in Table-1. Poor linear regression coefficients (R^2) values of less than 0.60 and high values of error function indicates the inapplicability of Pseudo-first-order kinetic model whereas high values of linear regression coefficients (R^2) of above 0.99 and low Chi square (χ^2) error values of less than 0.028 suggest the applicability of pseudo-second-order kinetic model (Table-1). Further, the calculated (q_e) for Pseudo-second order model for both adsorbates were

almost equivalent to the experimental (q_e) values. Applicability of Pseudo-second order kinetics model indicates that the rate limiting step is chemisorption (Afroze et al., 2016). On the other hand, intra-particle adsorption process parameters were obtained from fitting of plot of q_t (mg/g) vs. $t^{0.5}$ ($min^{0.5}$) as per equation (7) with the experimental data for which plots are not presented here. It was also found that none of these plots give linear straight line segment passing through the origin and hence indicates both the film diffusion and intra-particle diffusion occurred simultaneously and the adsorption of MB dye and Ni (II) onto pine cone bio-char particles may be controlled by film diffusion at earlier stages. Basically, adsorbate molecules move from bulk solution to the surface of the sorbent, through the boundary layer followed by mesopores intra-particle diffusion into the interior of the sorbent. From, Table.1, it was further observed that K_{id} (mg/g $min^{0.5}$) and constant (C) increased with the increases of initial adsorbate concentration, solution pH and temperature. Higher C values indicate greater boundary layer effect which suggests a higher contribution of the surface sorption in the rate limiting step.

2.5 Adsorption equilibrium isotherm study

Equilibrium isotherm study is very important to identify the mechanism of adsorption, determination of adsorbent's capacity as well as designing and operating the adsorption process.

Freundlich model was developed to explain how adsorption takes place on heterogeneous surface and the isotherm model assumes that the surface sites of the adsorbent have different biding energies (Dawood and Sen, 2012). The linearized form of Freundlich isother is represented as follows

$$\ln q_e = (1/n) \ln C_e + \ln k_f \quad (9)$$

Where q_e (mg/g) is the amount of adsorbate adsorbed at equilibrium, Ce is equilibrium adsorbate concentration (mg/L). K_f (L/g) is the Freundlich adsorption parameter and (n) is the surface heterogeneity factor which can be obtained from intercept and slope of a linear plot ln q_e vs ln C_e . Also for favourable adsorption n should be > 1. Freundlich model equation (9) was fitted well to our isotherm experimental results and high linear regression coefficients (R^2 = 0.96, 0.94) values are obtained for both Ni(II)-Pine char and MB-pine char system. Freundlich constants, K_f (L/g) were found to be 16.68 and 23.19 for Ni(II)-char and MB-Char systems respectively. The values of 'n' were observed to be greater than unity for both the systems which suggest that the adsorption process was favourable.

Langmuir isotherm model was developed in 1916 (Langmuir, 1916) to explain how adsorption takes place on homogeneous surfaces. The following linearized form of Langmuir model equation (10) which was fitted with isotherm experimental data

$$\frac{C_e}{q_e} = \frac{C_e}{q_m} + \frac{1}{K_L\, q_m} \qquad (10)$$

The maximum adsorption capacity q_m (mg/g) and Langmuir constant related to the energy of adsorption K_L (L/mg) were calculated from the slope and intercept of plot between C_e/q_e versus Ce. Again, very high values of linear regression coefficients ($R^2 >$ 0.99) indicates its applicability to isotherm study.

The Langmuir monolayer maximum adsorption capacity q_m (mg/g) for Ni (II) ions and MB dye were calculated as 117.65 and 106.38 (mg/g) respectively. This adsorption capacity of pine cone biochar is comparative with other biomass based bio-char such as

eucalyptus bark bio-char (104 mg/g), powdered active carbon (91 mg/g) ,Citrus Limettioides peel carbon (38.5 mg/g) and bamboo charcoal (53 mg/g).

4 Conclusion

The present study showed that cost effective pine cone based biochar was an effective adsorbent for the removal of aqueous phase MB dye and Ni(II) by adsorption. The kinetic data were analysed by using pseudo-first-order, pseudo-second-order and intra-particle diffusion model and mechanism and various kinetic model parameters were identified. Both Freundlich and Langmuir isotherm models were found to be applicable in describing the MB and Ni(II) adsorption onto biochar. Thermodynamic parameters suggested that the adsorption was an endothermic and spontaneous. These results indicated the applicability of pine cone as an economical precursor for the production of effective bio-char adsorbent.

Acknowledgement

Authors acknowledge the Chemical Eng department of Curtin University, Perth for providing necessary research infrastructure.

References

Afroze, S., Sen, T.K., Ang, H.M. 2016. Adsorption removal of zinc (II) from aqueous phase by raw and base modified Eucalyptus sheathiana bark: Kinetics, mechanism and equilibrium study. *Process Safety and Environmental Protection*, **102**, 336-352.

Dawood, S., Sen, T.K. 2012. Removal of anionic dye Congo red from aqueous solution by raw pine and acid-treated pine cone powder as adsorbent: Equilibrium,

293 thermodynamic, kinetics, mechanism and process design. *Water Research*,
294 **46**(6), 1933-1946.
295 Dawood, S., Sen, T.K., Phan, C. 2016. Adsorption removal of Methylene Blue (MB)
296 dye from aqueous solution by bio-char prepared from Eucalyptus sheathiana
297 bark: kinetic, equilibrium, mechanism, thermodynamic and process design.
298 *Desalination and Water Treatment*, **57**(59), 28964-28980.
299 Dawood, S., Sen, T.K., Phan, C. 2014. Synthesis and characterisation of novel-activated
300 carbon from waste biomass pine cone and its application in the removal of congo
301 red dye from aqueous solution by adsorption. *Water, Air, and Soil Pollution*,
302 **225**(1).
303 Hardy, B., Leifeld, J., Knicker, H., Dufey, J.E., Deforce, K., Cornélis, J.-T. 2017. Long
304 term change in chemical properties of preindustrial charcoal particles aged in
305 forest and agricultural temperate soil. *Organic Geochemistry*, **107**, 33-45.
306 Johari, K., Saman, N., Song, S.T., Cheu, S.C., Kong, H., Mat, H. 2016. Development of
307 coconut pith chars towards high elemental mercury adsorption performance –
308 Effect of pyrolysis temperatures. *Chemosphere*, **156**, 56-68.
309 Kara, İ., Yilmazer, D., Akar, S.T. 2017. Metakaolin based geopolymer as an effective
310 adsorbent for adsorption of zinc(II) and nickel(II) ions from aqueous solutions.
311 *Applied Clay Science*, **139**, 54-63.
312 Kılıç, M., Kırbıyık, Ç., Çepelioğullar, Ö., Pütün, A.E. 2013. Adsorption of heavy metal
313 ions from aqueous solutions by bio-char, a by-product of pyrolysis. *Applied*
314 *Surface Science*, **283**, 856-862.

315 Langmuir, I. 1916. The constitution and fundamental properties of solids and liquids.
316 Part I. Solids. *The Journal of the American Chemical Society*, **38**(2), 2221-2295.
317 Liao, P., Malik Ismael, Z., Zhang, W., Yuan, S., Tong, M., Wang, K., Bao, J. 2012.
318 Adsorption of dyes from aqueous solutions by microwave modified bamboo
319 charcoal. *Chemical Engineering Journal*, **195–196**, 339-346.
320 Maneerung, T., Liew, J., Dai, Y., Kawi, S., Chong, C., Wang, C.-H. 2016. Activated
321 carbon derived from carbon residue from biomass gasification and its application
322 for dye adsorption: Kinetics, isotherms and thermodynamic studies. *Bioresource*
323 *Technology*, **200**, 350-359.
324 Nawaz, S., Bhatti, H.N., Bokhari, T.H., Sadaf, S. 2014. Removal of Novacron Golden
325 Yellow dye from aqueous solutions by low-cost agricultural waste: Batch and
326 fixed bed study. *Chemistry and Ecology*, **30**(1), 52-65.
327 Nomura, S., Nishioka, H., Sen, T.K. 2017. Synthesis and Arsenic Adsorptive
328 Characteristics of a Novel Magnetic Adsorbent. *Journal of Environmental*
329 *Conservation Engineering*, **46**(3), 35-42.
330 Ribas, M.C., Adebayo, M.A., Prola, L.D.T., Lima, E.C., Cataluña, R., Feris, L.A.,
331 Puchana-Rosero, M.J., Machado, F.M., Pavan, F.A., Calvete, T. 2014.
332 Comparison of a homemade cocoa shell activated carbon with commercial
333 activated carbon for the removal of reactive violet 5 dye from aqueous solutions.
334 *Chemical Engineering Journal*, **248**(0), 315-326.
335 Sewu, D.D., Boakye, P., Woo, S.H. 2017. Highly efficient adsorption of cationic dye by
336 biochar produced with Korean cabbage waste. *Bioresource Technology*, **224**,
337 206-213.

338 Weber, J., Morriss, J.C. 1963. Kinetics of adsorption on carbonfrom solution. *J. Saint.*
339 *Eng. Div. Am. Soc. Civ. Eng*, **89**, 31-60.
340 Zhang, T., Zhu, X., Shi, L., Li, J., Li, S., Lü, J., Li, Y. 2017. Efficient removal of lead
341 from solution by celery-derived biochars rich in alkaline minerals. *Bioresource*
342 *Technology*, **235**, 185-192.
343 Zhou, N., Chen, H., Xi, J., Yao, D., Zhou, Z., Tian, Y., Lu, X. 2017. Biochars with
344 excellent Pb(II) adsorption property produced from fresh and dehydrated banana
345 peels via hydrothermal carbonization. *Bioresource Technology*, **232**, 204-210.

346 **Figures caption**

347 **Fig.1.** (a) Effect of initial solution pH on the adsorption of MB dye and Ni (II) onto pine
348 bio-char. (b) Effect of adsorbent dosage on the adsorption of MB dye and Ni (II). (c)
349 Effect of initial MB dye and Ni (II) concentration and (d) Effect of contact time on
350 initial MB dye adsorption. Where V= 50 ml, T=35 °C and Shaker Speed 130 rpm.

351

352

353

MB dye

Ni (II) ions

354

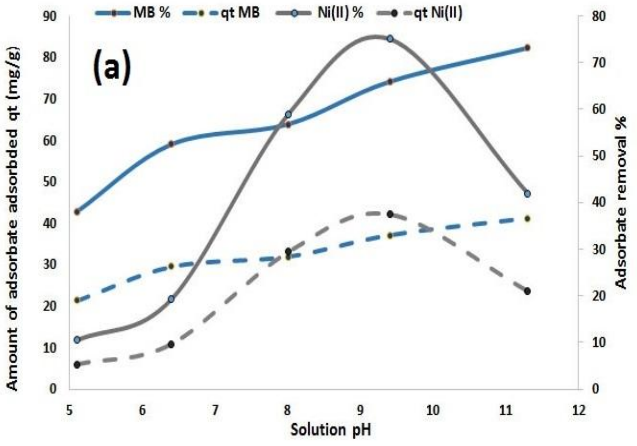

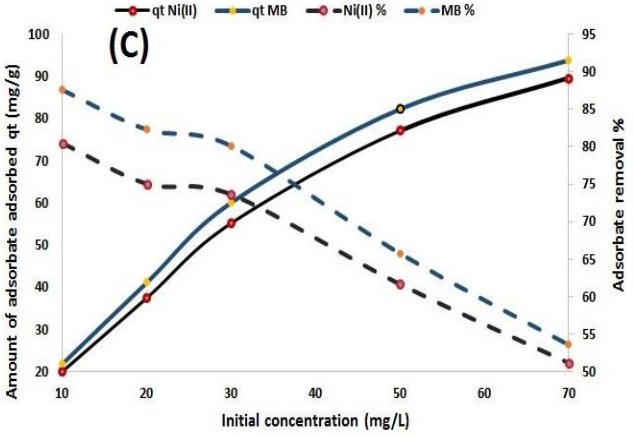

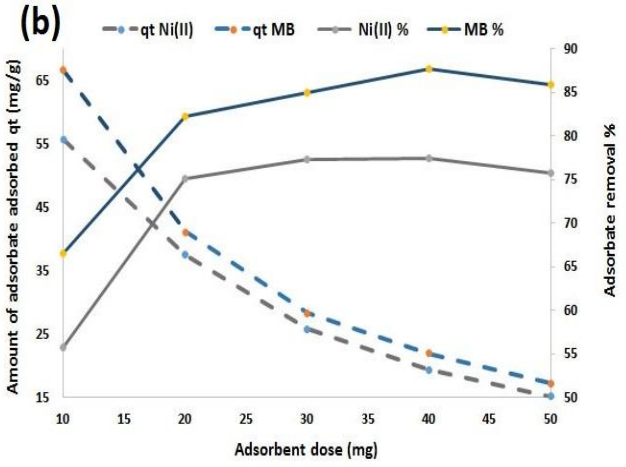

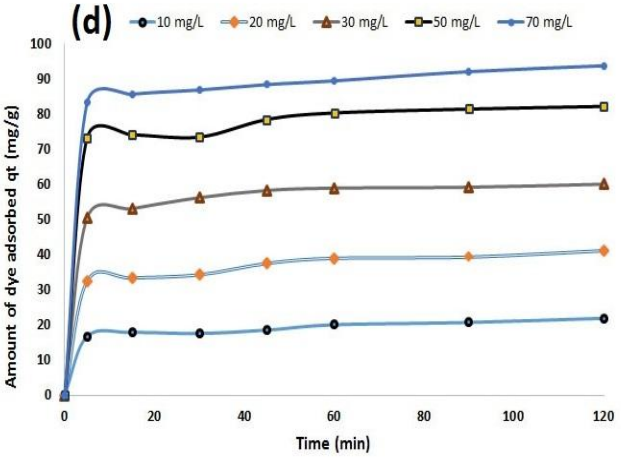

355

356

357

358

359

360

	Pseudo-second order					Intra-particle diffusion		Pseudo-second order					Intra-particle diffusion	
	q_e (mg/g), Exp	Ks (g/mg-min)	q_e (mg/g), Cal	χ^2	R^2	K_{id} (mg/g $min^{0.5}$)	C	q_e (mg/g), Expe	Ks (g/mg-min)	q_e (mg/g), Cal	χ^2	R^2	K_{id} (mg/g $min^{0.5}$)	C
Pine cone bio-char Dosage (mg)														
10	55.7	0.01	55.9	0.000	0.993	3.7	24.7	66.6	0.004	66.2	0.002	0.993	4.4	25.7
20	37.5	0.02	37.7	0.001	0.999	2.5	16.7	41.1	0.008	41.2	0.000	0.997	2.9	15.4
30	25.8	0.04	25.8	0.000	0.997	1.7	12.0	28.3	0.013	28.3	0.000	0.997	2.0	10.8
40	19.4	0.05	19.4	0.000	0.999	1.3	9.0	21.9	0.024	22.2	0.003	0.999	1.5	9.0
50	15.2	0.07	15.2	0.000	0.996	1.0	7.0	17.2	0.029	17.4	0.003	0.999	1.2	7.0
Initial Concentration (mg/L)														
10	20.11	0.077	20.12	0.000	0.999	1.3	9.6	21.9	0.011	21.7	0.003	0.995	1.5	7.9
20	37.52	0.018	37.74	0.001	0.999	2.5	16.7	41.1	0.008	41.2	0.000	0.997	2.9	15.4
30	55.21	0.035	55.25	0.000	0.999	3.6	26.1	60.1	0.013	60.2	0.001	0.999	4.1	25.6
50	77.11	0.188	76.92	0.000	0.999	4.8	39.6	82.2	0.008	82.6	0.002	0.999	5.5	36.2
70	89.63	0.139	89.29	0.001	0.999	5.5	45.9	93.8	0.007	93.5	0.001	0.999	6.1	41.9
pH														
5.1	5.24	0.293	5.24	0.000	0.999	0.3	2.5	21.4	0.018	21.6	0.001	0.997	1.5	8.6
6.4	9.64	0.021	9.80	0.003	0.995	0.7	2.9	29.5	0.011	29.7	0.001	0.997	2.1	10.9
8	29.40	0.009	29.76	0.004	0.997	2.2	10.1	31.9	0.006	32.9	0.028	0.991	2.4	9.8
9.4	37.52	0.018	37.74	0.001	0.999	2.5	16.7	37.1	0.007	37.2	0.000	0.996	2.6	13.0
11.3	20.97	0.035	21.01	0.000	0.999	1.4	9.1	41.1	0.008	41.2	0.000	0.997	2.9	15.4
Temperature														
25^0 C	30.590	0.018	30.77	0.001	0.999	2.1	13.1	28.8	0.021	28.6	0.001	0.998	1.8	12.9
35^0 C	37.519	0.018	37.74	0.001	0.999	2.5	16.7	41.1	0.008	41.2	0.000	0.997	2.9	15.4
45^0 C	39.110	0.018	39.37	0.002	0.999	2.6	17.5	41.8	0.007	41.8	0.000	0.996	2.9	15.4

Table 1 pseudo-second order and intra-particle diffusion model parameters for adsorption of ni (ii) and mb dye on pine cone bio-char

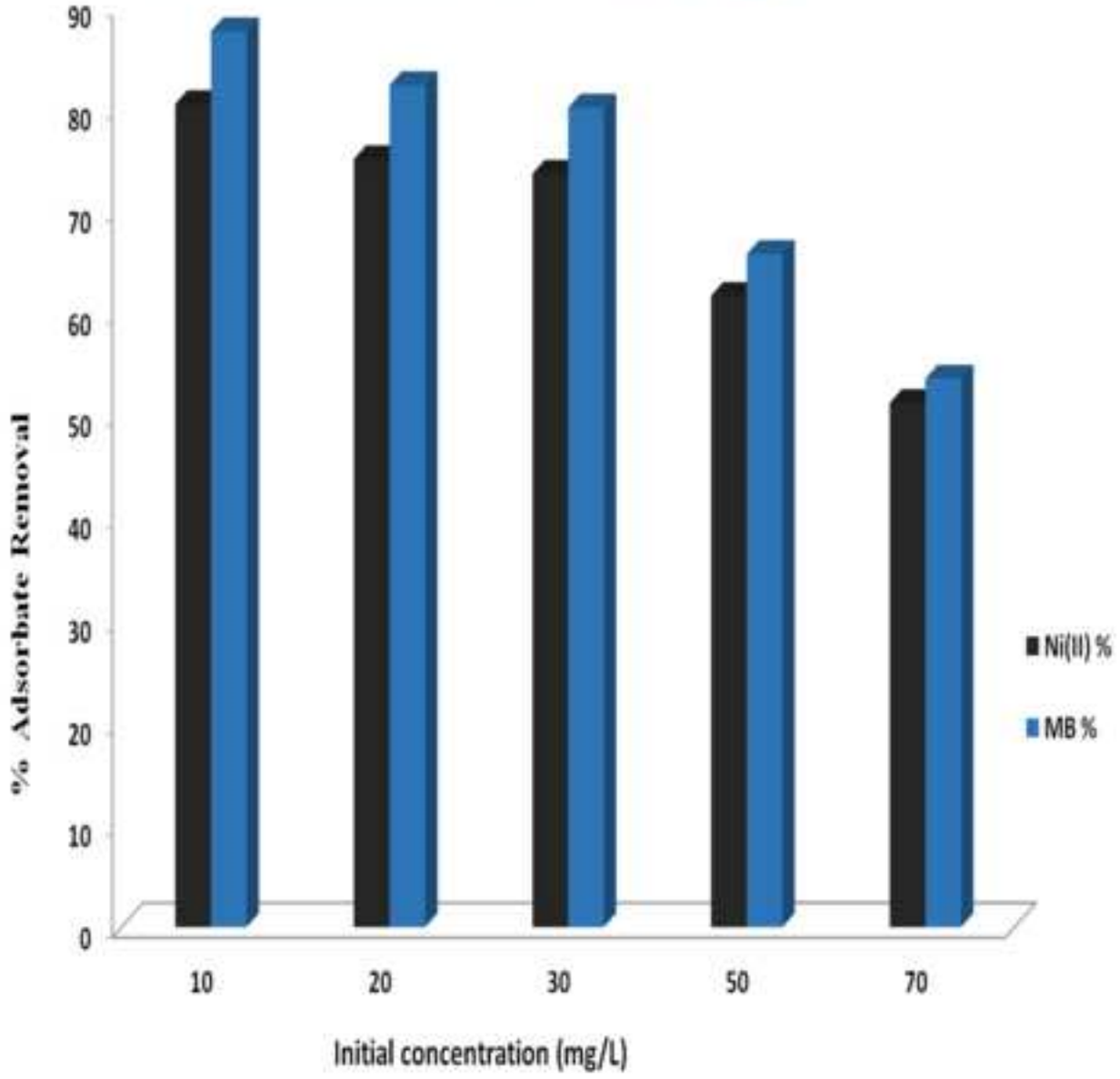

Highlights

- Pine cone based biochar adsorbent has been synthesized and characterized
- Removal of aqueous phase Ni(II) and MB by biochar has been studied
- Various physico-chemical factors on metal ions and dye adsorption has been analysed
- Mechanism of adsorption has been identified by kinetics and equilibrium studies.
- Pine cone as a cheap precursor for the sustainable production of bio-char adsorbent.